24. K. Siwicki, personal communication.
25. W. J. Joiner, A. Crocker, B. H. White, A. Sehgal, *Nature* 441, 757 (2006).
26. J. L. Pitman, J. J. McGill, K. P. Keegan, R. Allada, *Nature* 441, 753 (2006).
27. We thank J. Fitzgerald, H. Makarenkova, E. Frey, and R. Greenspan for helpful comments and input and K. Siwicki for expertise on the courtship assay. This work was supported by the NSF grant 0523216, the Neurosciences Research Foundation, and NIH grant R01-NS051305-01A1. All experiments except the courtship conditioning assay were conducted by I.G.-F.; the courtship conditioning experiment was conducted by J.D. The scope of the project and preparation of the manuscript were the result of a collaboration between I.G.-F. and P.J.S.

Supporting Online Material
www.sciencemag.org/cgi/content/full/313/5794/1775/DC1
Materials and Methods
Figs. S1 to S4
References and Notes

24 May 2006; accepted 1 August 2006
10.1126/science.1130408

Exogenous Induction of Cerebral β-Amyloidogenesis Is Governed by Agent and Host

Melanie Meyer-Luehmann,[1*] Janaky Coomaraswamy,[1*] Tristan Bolmont,[1,2*] Stephan Kaeser,[1] Claudia Schaefer,[1] Ellen Kilger,[1] Anton Neuenschwander,[3] Dorothee Abramowski,[3] Peter Frey,[3] Anneliese L. Jaton,[3] Jean-Marie Vigouret,[3] Paolo Paganetti,[3] Dominic M. Walsh,[4] Paul M. Mathews,[5] Jorge Ghiso,[6] Matthias Staufenbiel,[3] Lary C. Walker,[7]† Mathias Jucker[1,2]†

Protein aggregation is an established pathogenic mechanism in Alzheimer's disease, but little is known about the initiation of this process in vivo. Intracerebral injection of dilute, amyloid-β (Aβ)–containing brain extracts from humans with Alzheimer's disease or β-amyloid precursor protein (APP) transgenic mice induced cerebral β-amyloidosis and associated pathology in APP transgenic mice in a time- and concentration-dependent manner. The seeding activity of brain extracts was reduced or abolished by Aβ immunodepletion, protein denaturation, or by Aβ immunization of the host. The phenotype of the exogenously induced amyloidosis depended on both the host and the source of the agent, suggesting the existence of polymorphic Aβ strains with varying biological activities reminiscent of prion strains.

The accumulation of misfolded proteins is a common feature of several neurodegenerative disorders. In Alzheimer's disease (AD), the multimerization of the Aβ peptide is an early and central process in the pathogenic cascade (*1*–*3*), but little is known about the mechanisms that govern the initiation of Aβ aggregation and deposition in vivo. Ordered protein aggregation in vitro is a function of protein concentration and time and follows a crystallization-like polymerization mechanism that can be rapidly initiated by introducing an exogenous seed (*4*). In vivo, seeded aggregation of Aβ is seen after injecting AD brain extracts into the brains of non-human primates (*5*) or APP-transgenic mice (*6*), reminiscent of the conformational conversion mechanism of prion infectivity (*7*–*9*).

We injected 10% (w/v) extracts of brain homogenates from autopsied AD patients (AD extract) or from aged, β-amyloid–laden APP23 transgenic mice (*10*) (APP23 Tg extract) into the hippocampus of young male APP23 mice. Four months later, the host mice were analyzed (*11*). Both AD extract and APP23 Tg extract induced robust deposition of Aβ in the hippocampus (Fig. 1, A and B). Intracerebral injection of tissue extract from an aged control patient induced only minimal Aβ deposits, consistent with the low Aβ load in the donor (Fig. 1C; fig S1). No seeded Aβ deposits were found after control injections of brain extract from an aged, wild-type mouse or of phosphate-buffered saline (PBS) (Fig. 1, D and E). Infusion of APP23 Tg extract into wild-type mice did not induce Aβ deposition; thus, the observed Aβ deposits did not simply represent the

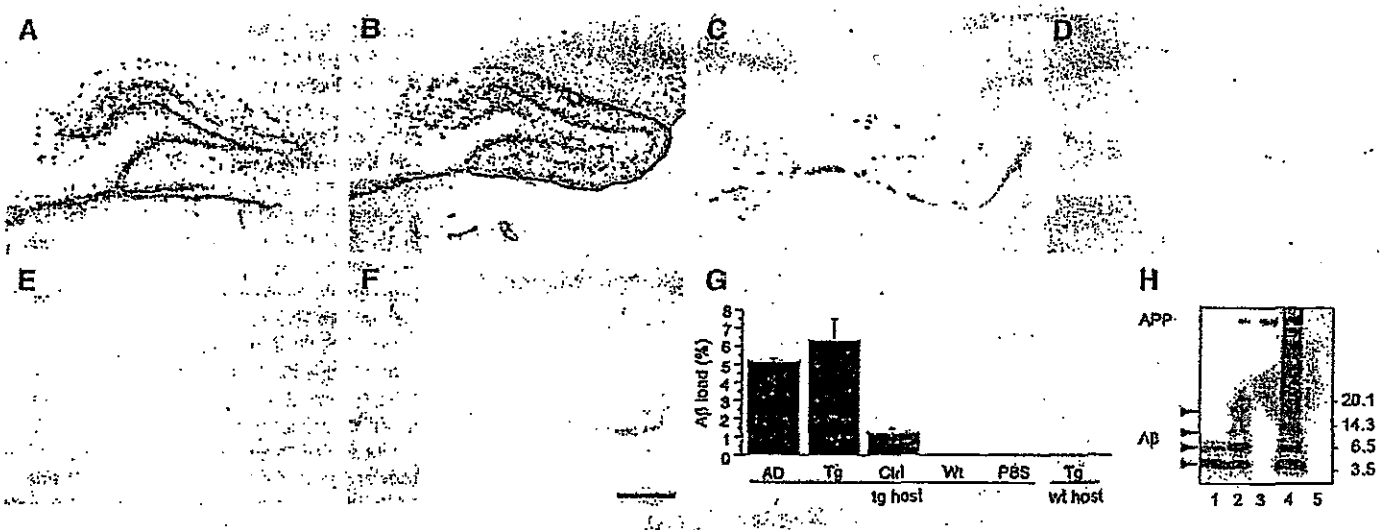

Fig. 1. Brain extract (10%) was injected into the hippocampus of 5-month-old male APP23 hosts (A to E) and nontransgenic littermates (F). Mice were analyzed 4 months later. Injection of AD extract (A) and APP23 Tg brain extract (B) induced numerous Aβ-immunoreactive deposits. Few or no Aβ deposits were detected after injections of brain extract from an aged (95 years) control (Ctrl) patient (C) or wild-type (Wt) mouse (D). No Aβ deposits were observed after PBS injections (E) or when Tg extract was injected into wild-type mice (F). Stereological quantification of Aβ load by immunohistochemistry (G) confirmed significant amyloid induction by AD and Tg brain extracts compared to Ctrl and Wt extracts ($n = 5$ mice per group; mean ± SEM, $P < 0.001$). (H) Tris-Tricine SDS–polyacrylamide gel electrophoresis (PAGE) followed by immunoblotting with a human Aβ-specific antibody. Lane 1: synthetic Aβ1-40 + Aβ1-42 (1 ng/μl each); lane 2: AD brain extract; lane 3: Ctrl brain extract; lane 4: APP23 Tg brain extract; and lane 5: Wt brain extract. For each extract, 1 μl was loaded. Arrowheads indicate monomeric, dimeric, trimeric, and tetrameric Aβ. Aβ concentration in the control patient extract was below the detection level. When less dilute samples were used, Aβ was detected in the Ctrl extract, consistent with the sparse amyloid plaques in this patient (fig. S1) and the modest seeding activity of the Ctrl extract. Scale bar, 350 μm.

injected Aβ-containing material (Fig. 1F), and imply that host factors are critical for in vivo seeding. No seeded Aβ deposits were observed when APP23 Tg extract from a young, 2-month-old, predepositing mouse was injected into APP23 hosts. The concentrations of Aβ in the AD and APP23 Tg extracts were estimated to be 1 to 10 ng/μl. In both AD extract and APP23 Tg extract, Aβ monomers, oligomers, and larger multimeric species were present (Fig. 1H).

The localization and biochemical nature of the induced Aβ lesions were markedly similar to those seen in normal, aged APP23 transgenic mice (*10*, *12*). Induced Aβ deposits were found primarily in the injected hippocampus, but some were also observed in the dorsal lateral geniculate nucleus, corpus callosum, and entorhinal cortex, and in the vasculature of the thalamus and pia mater (fig. S2). Most induced Aβ deposits were diffuse, although some congophilic amyloid plaques were present and surrounded by activated microglia, astrocytes, and dystrophic neurites (fig. S2). Aβ in micropunches taken from the hippocampus of injected APP23 mice was mainly parechymal and consisted of Aβ1-40 and Aβ1-42, whereas the amyloid in the thalamic micropunches was mostly vascular and consisted predominantly of Aβ1-40 (fig. S3).

The exogenous induction of Aβ deposition in vivo also is time and concentration dependent (fig. S4). Immunoreactive Aβ deposits first appeared 2 months after injection and thereafter increased significantly with time. APP23 extract that was further diluted to 0.5% produced a pattern of deposition in the host similar to that seen with the 10% extract, but with much less potency (fig. S4).

The phenotype of exogenously induced β-amyloid deposits is dependent on both the agent and the host. We injected brain extract from aged APP23 mice into APP–presenilin-1 (PS1) transgenic hosts, and vice versa (Fig. 2). Amyloid deposition in the hippocampus of male APP23 mice normally begins at 9 to 10 months of age, whereas APPPS1 mice develop Aβ deposition in the hippocampus at 3 to 4 months of age (*10*, *13*). Total Aβ concentration was similar in the two extracts (Fig. 2I), but in APPPS1 extracts, the highly amyloidogenic Aβ1-42 was several times as abundant as Aβ1-40, whereas in extracts from

[1]Department of Cellular Neurology, Hertie-Institute for Clinical Brain Research, University of Tübingen, D-72076 Tübingen, Germany. [2]Institute of Pathology, University of Basel, CH-4003 Basel, Switzerland. [3]Novartis Institutes for Biomedical Research, CH-4002 Basel, Switzerland. [4]Conway Institute of Biomolecular and Biomedical Research, University College Dublin, Dublin, Republic of Ireland. [5]Nathan Kline Institute, New York University School of Medicine, Orangeburg, NY 10962, USA. [6]Departments of Pathology and Psychiatry, New York University School of Medicine, New York, NY 10016, USA. [7]Yerkes National Primate Research Center and Department of Neurology, Emory University, Atlanta, GA 30322, USA.

*These authors contributed equally to this work.
†To whom correspondence should be addressed. E-mail: mathias.jucker@uni-tuebingen.de (M.J.); lary.walker@emory.edu (L.C.W.)

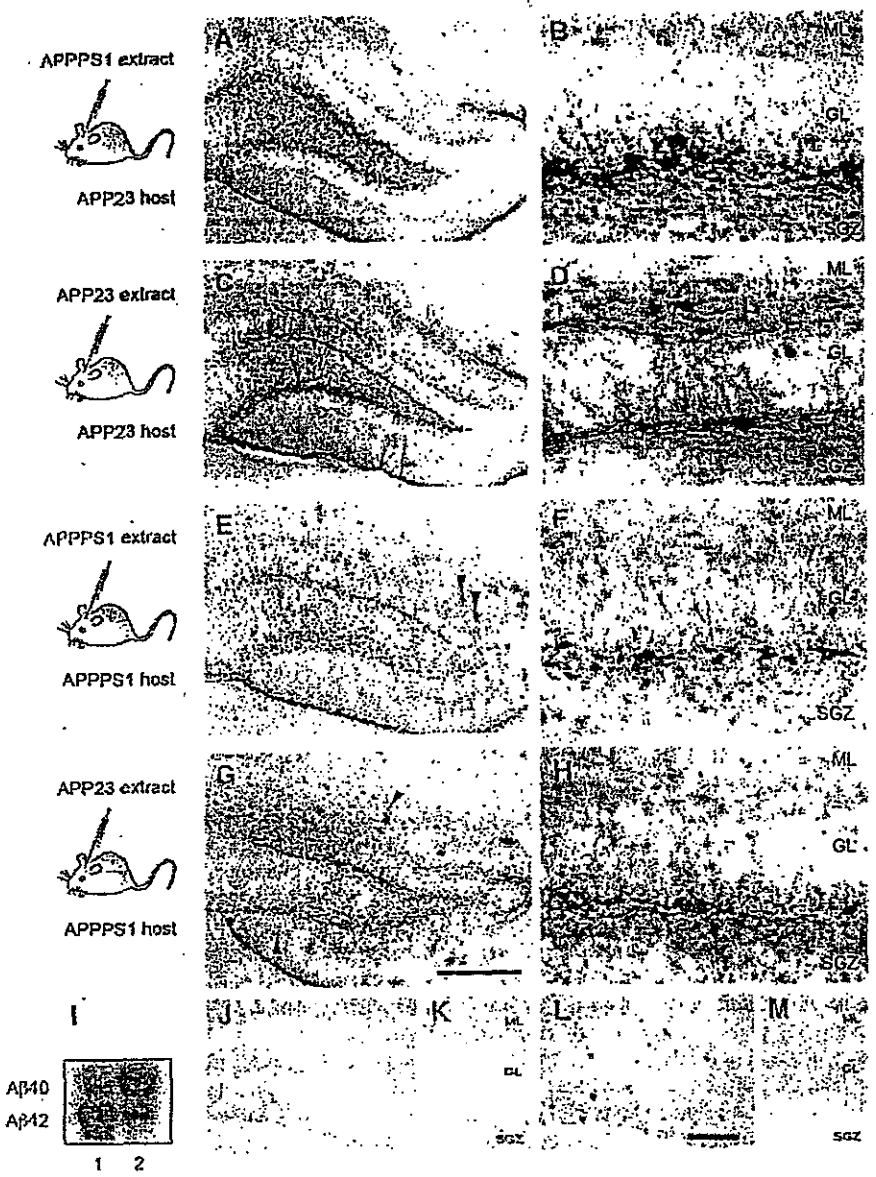

Fig. 2. Brain extract (10%) from an aged APPPS1 mouse or an aged APP23 mouse was injected intrahippocampally into either 5-month-old male APP23 or 2-month-old male APPPS1 hosts. Brains were immunohistochemically analyzed for Aβ 3 months later. The panels to the left (A, C, E, and G) show overviews of the hippocampus, and the panels to the right (B, D, F, and H) show corresponding higher magnification images of the upper blade of the dentate gyrus (ML, molecular layer; GL, granular cell layer; SGZ, subgranular cell layer). The coarse, punctate pattern of Aβ staining in the APP23 host is apparent, particularly in the SGZ, after injection of the APPPS1 extract (A and B). Injection of APP23 extract induced more filamentous and diffuse Aβ in the ML (C and D). When APPPS1 extract was injected into the APPPS1 host, the coarse, punctate pattern of Aβ induction was even more distinct (E and F), whereas the APP23 extract in APPPS1 hosts induced Aβ lesions intermediate in appearance to the coarse and filamentous types (G and H). At 5 months of age, APPPS1 hosts had developed some Aβ deposits endogenously, predominantly in the ML [arrowheads in (E) and (G)]. For comparison, an 8-month-old noninjected male APP23 mouse (J and K) and a 5-month-old noninjected male APPPS1 mouse (L and M) are shown. Scale bar, 350 μm. (I) Urea-based SDS-PAGE immunoblot analysis with an antibody specific to human Aβ. Lane 1: APPPS1 extract; lane 2: APP23 extract. Aβ1-42 was the major Aβ species in APPPS1 mice, whereas Aβ1-40 predominated in the APP23 extract. Total Aβ was comparable in the two extracts [APPPS1: total Aβ, 14.7 ng/μl (Aβ40: 4.6 ng/μl; Aβ42: 10.1 ng/μl); and APP23: total Aβ, 11.7 ng/μl (Aβ40: 8.1 ng/μl; Aβ42: 3.6 ng/μl)].

APP23 mice, more Aβ1-40 was present. The amyloid-inducing activity of APP23 and APPPS1 extracts was quantitatively similar 3 months after infusion, but injection of APPPS1 extract into APP23 hosts consistently induced a coarse pattern of compact, punctate Aβ deposition that was mainly confined to the subgranular layer of the hippocampus, whereas the APP23 extract injected into APP23 hosts yielded primarily diffuse and filamentous lesions, with substantial diffuse Aβ in the molecular layer (Fig. 2, A to D). When the same extracts were injected into the APPPS1 host, lesions induced by the APPPS1 extract were even more coarse and punctate, whereas those induced by the APP23 extract were a mixture of filamentous and compact types (Fig. 2, E to H). In mice analyzed 1 month after the infusion of the extract, appreciable coarse Aβ induction was already apparent in APPPS1 hosts but not in APP23 hosts.

To establish whether Aβ is a prerequisite for the amyloid-inducing activity of the extract, APP23 Tg extracts were either Aβ-immunodepleted (Fig. 3, A to C) or mixed with the Aβ-specific antibody (anti-Aβ) Beta-1 (Fig. 3, D to F) and injected into young APP23 hosts. Immunodepletion completely prevented the amyloid-inducing activity of the extract, whereas the Beta-1–containing extract attenuated amyloid induction by >60% compared to a control antibody.

Passive immunization of APP23 host mice with Beta-1 antibodies inhibited the development of induced lesions. Administration of the antibodies commenced 4 weeks after the intracerebral injection of APP23 Tg extract in order not to interfere with the initial seeding process. Serum anti-Aβ titers of 1:2400 to 1:8000 were maintained until mice were killed 4 months after the extract infusion. Amyloid induction was almost completely inhibited in immunized mice compared to those injected with control antibody

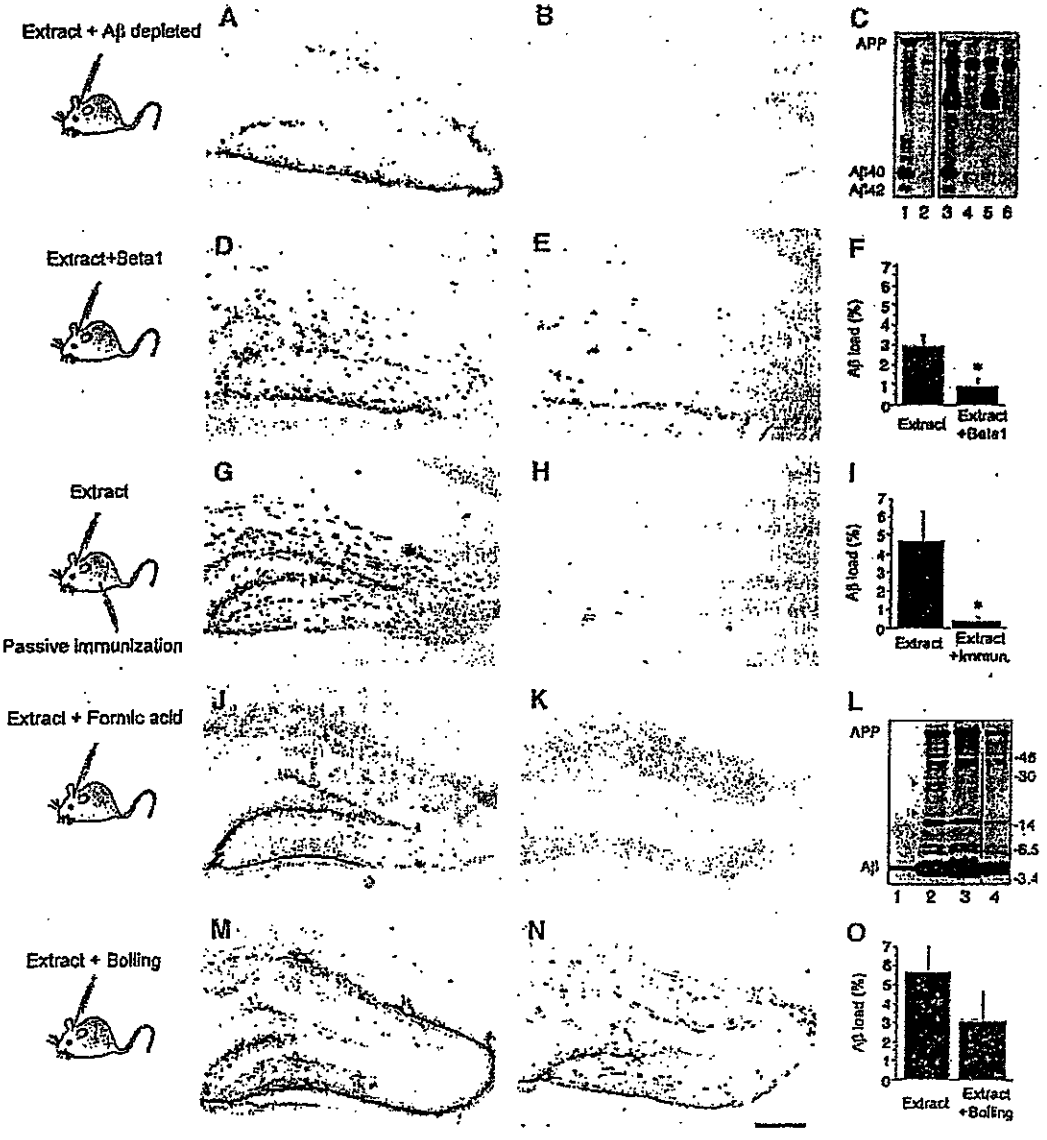

Fig. 3. (A to C) Immunodepletion: APP23 Tg brain (0.5%) extract (A) or the same extract Aβ-immunodepleted (B) was injected intrahippocampally into 3-month-old APP23 mice that were then analyzed 3 months later. Immunodepletion completely eliminated the amyloid-inducing activity of the extract. (C) Urea-based SDS-PAGE followed by immunoblotting with human Aβ-specific antibody. Lane 1: intact APP23 Tg extract; lane 2: immunodepleted extract (the absence of detectable Aβ and APP fragments is apparent); lanes 3 to 6: eluted pellet fractions after the first, second, third, and fourth depletion steps. (D to F) Antibody blocking: APP23 or AD brain extract (10%) was mixed with either a control antibody or with anti-Aβ Beta-1 and injected into 6-month-old male APP23 mice. Four months after injection, amyloid induction was significantly lower in the Beta-1–injected mice (E) than in the control mice (D), as confirmed by stereological quantification of immunoreactive Aβ (F) ($n = 5$ mice per group; $P < 0.05$). (G to I) Immunization: APP23 or AD brain extract (10%) was injected intrahippocampally into 6-month-old male APP23 mice, followed by weekly peripheral injections of Beta-1 antibody (H) or control antibody (G), starting 1 month after the brain-extract injections. Four months later, immunohistochemical (G and H) and stereological (I) analysis revealed a >90% inhibition of amyloid induction by passive immunization ($n = 5$ mice per group; $P < 0.001$). (J to L) Formic acid treatment: APP23 Tg extract (10%) was treated with formic acid and injected into the hippocampus of 3-month-old APP23 mice that were analyzed 3 months later. (K) Formic acid completely nullified the amyloid-inducing activity of the extract. (J) PBS-treated control extract. (L) Bicine-Tris SDS-PAGE (without urea) followed by immunoblot analysis with human Aβ-specific antibodies. Lane 1: synthetic Aβ (2 ng/μl); lane 2: PBS-treated control APP23 extract (10 μl); and lanes 3 and 4: formic acid–treated APP23 extract (20 μl in lane 3 and 10 μl in lane 4). The oligomeric bands are absent or greatly reduced (arrowheads) in the formic acid–treated extract, even at twice the concentration of the control extract. (M to O) Heating: APP23 extract (10%) was heated to 95°C (N) before injection into the hippocampus of 3-month-old APP23 mice. Analysis 3 months later showed that heating reduced (45%) but did not eliminate Aβ seeding ($n = 3$ mice per group; $P > 0.05$). Scale bar, 350 μm.

(Fig. 3, G to I). An active immunization protocol revealed similar inhibition (fig. S5).

The amyloid-inducing activity of the extract was disrupted by formic acid denaturation. APP23 Tg extracts were treated for 1 hour with 70% formic acid, followed by dialysis, or heated to 95°C for 5 min, cooled, and injected into young APP23 mice. Formic acid treatment completely abolished the amyloid-inducing activity of the extract, whereas heating reduced, but did not eliminate, amyloid induction (Fig. 3, J to O).

Preparations of soluble or fibrillar synthetic Aβ40, Aβ42, or a mixture of both, in amounts similar to those of Aβ in APP23 Tg brain extracts, failed to induce detectable Aβ deposition (Fig. 4). Injection of synthetic Aβ at concentrations 100 to 1000 times that of Aβ in APP23 Tg brain extracts resulted in amorphous masses of material near the injection site that consisted primarily of the injected material. Few newly generated aggregates were present, as confirmed by infusion of biotinylated Aβ1-42 (fig. S6). Synthetic Aβ oligomers (*14–16*) also were ineffective at inducing parenchymal and vascular amyloid, as was Aβ isolated from the conditioned media of cells stably transfected with APP (table S1; fig. S6). Addition of cofactors such as ApoE4 and Cu/Zn, which are thought to promote the polymerization of Aβ (*17, 18*), did not augment the potency of synthetic material (table S1). Injection of synthetic Aβ mixed with brain extract from wild-type mice also did not produce notable β-amyloidosis (table S1). Finally, the possibility that poor seeding by synthetic Aβ results from the activation of the Aβ-degrading enzyme neprilysin (*19*) or a humoral immune response (*20*) was ruled out by unchanged neprilysin immunoreactivity and by the absence of serum anti-Aβ antibodies in mice injected with synthetic Aβ.

Thus, cerebral extracts induce Aβ deposition in vivo by supplementing (or anticipating) endogenously generated Aβ seeds with exogenous seeds that probably consist of a form of multimeric Aβ. The host-specific morphology and distribution of the induced lesions underscore the essential role of the host in regulating pathogenesis, but the inducing agent also contributes to the pathologic phenotype. The inhibition of seeding by specific immunoneutralization of Aβ (*20*) or formic acid denaturation of the extracts (*21*) suggests that the active agent consists of an aggregated Aβ species (*20, 21*). The finding that synthetic Aβ lacks amyloid-inducing activity in vivo was not unexpected, inasmuch as prion disease has also been difficult to transmit by in vitro–generated (recombinant) prions (*8*).

Synthetic and cell culture–derived Aβ, in concentrations similar to those tested in the present study, are neurotoxic in vivo (*14, 22, 23*) and can impair long-term potentiation and cognitive function (*24, 25*). These observations, in light of the highly variable seeding efficacy of in vitro and in vivo preparations, suggest the occurrence of various Aβ conformations with partially distinct biological activities (*26*), similar to prions (*27, 28*). Polymorphic and self-propagating synthetic Aβ strains recently have been reported (*9*). Thus, Aβ multimers in vivo also may be polymorphic and polyfunctional, again reminiscent of prions, in which infectivity is strain-dependent and fully encoded in distinct multidimensional conformations (*29*). Whether oligomeric forms of Aβ that are thought to be key cytoactive disease agents (*25, 30, 31*) can also be seeded in vivo remains to be determined.

There is currently no evidence that β-amyloidosis (and in particular AD) is transmissible in the same sense as are prion diseases, which can be transmitted to wild-type hosts via diverse routes of varying efficiency and involve systemic cellular mechanisms of prion uptake and distribution (*7, 32*). However, an understanding of the mechanisms involved in the instigation and propagation of abnormal Aβ assemblies in vivo could shed light on the origins of idiopathic Alzheimer's disease.

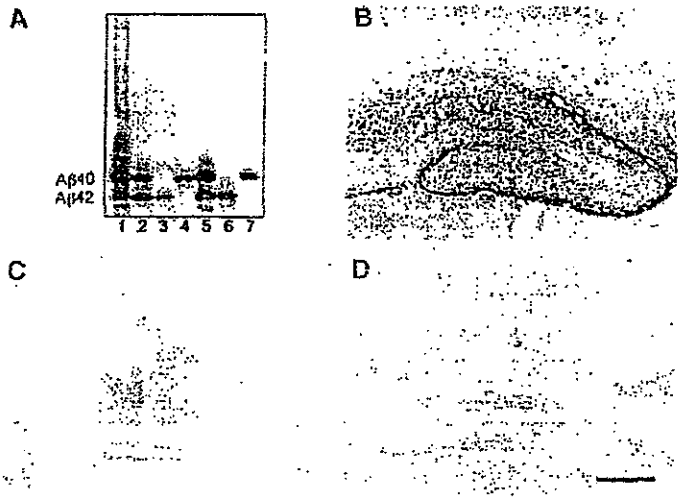

Fig. 4. Fresh and aged Aβ preparations were made from Aβ1-40 or Aβ1-42, or from a 2:1 mixture of Aβ1-40 and Aβ1-42 at ~5 ng/μl, similar to the Aβ concentrations in a 10% APP23 brain extract. (A) Urea-based SDS-PAGE followed by immunoblotting with a human Aβ-specific antibody. Lane 1: APP23 Tg brain extract; lane 2: mixed fresh Aβ1-40 + Aβ1-42; lane 3: fresh Aβ1-42; lane 4: fresh Aβ1-40; lane 5: aged Aβ1-40 + Aβ1-42; lane 6: aged Aβ1-42; and lane 7: aged Aβ1-40. Preparations were injected intrahippocampally into 5-month-old male APP23 mice that were analyzed 4 months later. The aged Aβ preparations were fibrillar in nature as verified by electron microscopy and Congo red binding (fig. S6). Multimeric Aβ species are not easily detected with this urea-based gel system, which is designed to separate the different Aβ isoforms. The additional band in the brain extract is likely Aβ1-38. (B) Amyloid induction with an APP23 Tg extract. (C and D) No induced Aβ deposits were detectable with any of the synthetic Aβ preparations at this concentration. Shown are animals injected with freshly mixed Aβ1-40 + Aβ1-42 (C) and aged Aβ1-40 + Aβ1-42 (D). Scale bar, 350 μm.

References and Notes

1. D. J. Selkoe, *Nature* 426, 900 (2003).
2. J. Hardy, D. J. Selkoe, *Science* 297, 353 (2002).
3. M. P. Mattson, *Nature* 430, 631 (2004).
4. J. D. Harper, P. T. Lansbury Jr., *Annu. Rev. Biochem.* 66, 385 (1997).
5. R. M. Ridley, H. F. Baker, C. P. Windle, R. M. Cummings, *J. Neural Transm.* 113, 1243 (2006).
6. M. D. Kane *et al.*, *J. Neurosci.* 20, 3606 (2000).
7. A. Aguzzi, C. Haass, *Science* 302, 814 (2003).
8. G. Legname *et al.*, *Science* 305, 673 (2004).
9. A. T. Petkova *et al.*, *Science* 307, 262 (2005).
10. C. Sturchler-Pierrat *et al.*, *Proc. Natl. Acad. Sci. U.S.A.* 94, 13287 (1997).
11. Materials and Methods are available as supporting material on *Science* Online.
12. M. E. Calhoun *et al.*, *Proc. Natl. Acad. Sci. U.S.A.* 96, 14088 (1999).
13. R. Radde *et al.*, *EMBO Rep.*, 7, 940 (2006).
14. S. Barghorn *et al.*, *J. Neurochem.* 95, 834 (2005).
15. C. G. Glabe, R. Kayed, *Neurology* 66, S74 (2006).
16. A. Schmechel *et al.*, *J. Biol. Chem.* 278, 35317 (2003).
17. R. A. Cherny *et al.*, *Neuron* 30, 665 (2001).
18. R. B. DeMattos, *J. Mol. Neurosci.* 23, 255 (2004).
19. M. H. Mohajeri, M. A. Wollmer, R. M. Nitsch, *J. Biol. Chem.* 277, 35460 (2002).
20. D. Schenk *et al.*, *Nature* 400, 173 (1999).
21. A. E. Roher *et al.*, *J. Biol. Chem.* 268, 3072 (1993).
22. C. Geula *et al.*, *Nat. Med.* 4, 827 (1998).
23. A. Stephan, S. Laroche, S. Davis, *J. Neurosci.* 21, 5703 (2001).
24. J. P. Cleary *et al.*, *Nat. Neurosci.* 8, 79 (2005).
25. D. M. Walsh *et al.*, *Nature* 416, 535 (2002).
26. A. Piccini *et al.*, *J. Biol. Chem.* 280, 34186 (2005).
27. P. Chien, J. S. Weissman, A. H. DePace, *Annu. Rev. Biochem.* 73, 617 (2004).
28. B. Chesebro *et al.*, *Science* 308, 1435 (2005).
29. E. M. Jones, W. K. Surewicz, *Cell* 121, 63 (2005).
30. M. P. Lambert *et al.*, *Proc. Natl. Acad. Sci. U.S.A.* 95, 6448 (1998).
31. S. Lesne *et al.*, *Nature* 440, 352 (2006).
32. M. Prinz *et al.*, *Nature* 425, 957 (2003).

33. We thank H. LeVine (Lexington), J. Hardy (Bethesda), M. Mattson (Baltimore), M. Tolnay (Basel), F. Heppner (Zürich), B. Sahagan (Groton), and D. Selkoe (Boston) for helpful discussions. Aβ preparations were provided by P. Palumaa (Tallinn), J. Fryer and D. Holtzman (St. Louis), G. Multhaup (Berlin), C. Glabe and R. Kayed (Irvine), and U. Ebert and H. Hillen (Ludwigshafen). Antibodies were provided by K. Beyreuther (Heidelberg). The help of R. Radde (Tübingen) is gratefully acknowledged. Supported by grants from the Alzheimer Association (IIRG-02-4127; ZEN-06-27341), Swiss National Science Foundation (3100-068329.02), European Union contract LSHM-CT-2003-503330 (APOPIS), and German National Genome Network (NGFN2) (to M.J.); the Wellcome Trust (067660) (to D.M.W.); the National Institute of Neurological Disorders and Stroke (NS45357) (to P.M.M.); and the NIH (RR-00165) (to L.C.W.).

Supporting Online Material

www.sciencemag.org/cgi/content/full/313/5794/1781/DC1
Material and Methods
Fig. S1 to S6
Table S1
References

28 June 2006; accepted 7 August 2006
10.1126/science.1131864

医薬品 研究報告 調査報告書

識別番号・報告回数			報告日	第一報入手日	新医薬品等の区分	機構処理欄
				2007. 2. 8	該当なし	

一般的名称	乾燥濃縮人血液凝固第Ⅷ因子	研究報告の公表状況	Tumpey TM, Maines TR, Van Hoeven N, Glaser L, Solorzano A, Pappas C, Cox NJ, Swayne DE, Palese P, Katz JM, Garcia-Sastre A. Science. 2007 Feb 2;315(5812):655-9.	公表国
販売名(企業名)	クロスエイトM250(日本赤十字社) クロスエイトM500(日本赤十字社) クロスエイトM1000(日本赤十字社)			米国

研究報告の概要	使用上の注意記載状況・その他参考事項等
○1918年のインフルエンザウイルスのヘマグルチニンの2つのアミノ酸の変化が伝播を終焉させた 1918年のインフルエンザパンデミックは、世界中に広まったウイルスの感染爆発による大災害であった。本稿は、この1918年インフルエンザのヘマグルチニン受容体の結合部位のごくわずかな変化により、ウイルスの伝播性が変化したことを示す。2つのアミノ酸変異によって、ウイルスの受容体への結合しやすさがヒトのα-2,6シアル酸からトリのα-2,3シアル酸へと転換すると、フェレット間で呼吸器飛沫による感染を起こさないウイルスとなったが、致死性および上気道での複製能は保持していた。さらに、α-2,6およびα-2,3双方に特異性のある1918年ウイルスは感染性が低いことから、ヒトのalpha-2,6シアル酸への結合優先性が、このパンデミックウイルスの至適感染に不可欠であることを示している。以上の知見は、ヘマグルチニン受容体の特異性が、哺乳類におけるインフルエンザ伝播に重要な役割を担うことを裏付けるものである。	クロスエイトM250 クロスエイトM500 クロスエイトM1000 血液を原料とすることに由来する感染症伝播等 vCJD等の伝播のリスク

報告企業の意見	今後の対応
1918年インフルエンザウイルスのヘマグルチニン受容体結合部位のごくわずかな変化により、ウイルスの伝播性が変化したとの報告である。	トリインフルエンザウイルスは脂質膜を持つRNAウイルスである。これまで、本製剤によるトリインフルエンザウイルス感染の報告はない。本製剤の製造工程には、平成11年8月30日付医薬発第1047号に沿ったウイルス・プロセスバリデーションによって検証された2つの異なるウイルス除去・不活化工程が含まれている。本製剤の安全性は確保されていると考えるが、トリインフルエンザは日本でも鶏から検出されており、流行した場合、献血者減少につながることも予想される。今後も引き続き情報の収集に努める。

reduced but not abolished, were not as sensitive as *rtt109Δ* cells (Fig. 3, A and B). Moreover, *rtt109Δ H3-K56R* and *rtt109Δ H3-K56A* double-mutant cells displayed similar sensitivities toward these DNA-damaging agents as either single mutant alone (Fig. 3A and fig. S5). In contrast, cells expressing *rtt109* site-specific mutants where H3-K56 acetylation was not affected were resistant to these DNA-damaging agents (Fig. 3B and fig. S6). These results suggest that the ability of Rtt109 to suppress sensitivity toward DNA-damaging agents is mainly mediated by its HAT activity toward H3-K56.

In budding yeast, Rad52 forms spontaneous foci, predominantly during S and G_2-M phases of the cell cycle, and these foci are thought to be sites of repair of DNA lesions (*18*, *19*). Cells with mutations in proteins involved in DNA metabolism, such as Top3 exhibit elevated levels of Rad52 foci, possibly due to an increase in spontaneous chromosome breaks (*20*). The *rtt109Δ* and *H3-K56R* single- and double-mutant cells showed a substantial increase in Rad52 fused with yellow fluorescent protein (Rad52-YFP) foci (Fig. 3, C and D). Moreover, the *rtt109Δ* H3-K56R double-mutant cells did not exhibit more Rad52 foci than either *rtt109Δ* or *H3-K56R* mutant alone (Fig. 3D). Thus, the increase in Rad52-YFP foci observed in *rtt109Δ* mutant cells appears mainly to be due to loss of H3-K56 acetylation. Supporting this idea, acetylation of four other H3 lysine residues (K9, K14, K18, and K23) was not altered in the *rtt109Δ* mutant cells (fig. S7). Taken together, these data indicate that Rtt109-mediated acetylation of H3-K56 during S phase protects DNA from damage.

Here we have shown that Rtt109 is a member of a novel HAT family that acetylates H3-K56. The *rtt109Δ* mutant exhibited a synthetic lethal or slow-growth phenotype with a mutant allele of PCNA (proliferating cell nuclear antigen), *pol30-79*, which is defective in DNA replication and repair (*21*), but not with the PCNA mutant allele, *pol30-8*, which is defective in epigenetic silencing (*22*) (fig. S8A). The *rtt109Δ* mutant also exhibited a synthetic lethal/slow growth phenotype with a mutation in DNA polymerase α (fig. S8B) and was previously found to genetically interact with Orc2 and Cdc45 mutations (*23*, *24*). All of these proteins are involved in DNA replication. The genetic interactions between Rtt109 and the proteins involved in DNA replication suggest that the *rtt109Δ* mutant cells are defective in certain aspects of DNA replication. In support of this idea, the *rtt109Δ* mutant exhibits synthetic lethal or slow-growth phenotypes with mutations in genes such as *RAD52*, which are involved in homologous recombination (*25*), a process that is needed to resolve stalled replication forks (*26*). Thus, H3-K56 acetylation by Rtt109 is closely linked to DNA replication.

References and Notes

1. J. Wu, M. Grunstein, *Trends Biochem. Sci.* **25**, 619 (2000).
2. T. Jenuwein, C. D. Allis, *Science* **293**, 1074 (2001).
3. Y. Zhang, D. Reinberg, *Genes Dev.* **15**, 2343 (2001).
4. B. D. Strahl, C. D. Allis, *Nature* **403**, 41 (2000).
5. M. J. Carrozza, R. T. Utley, J. L. Workman, J. Cote, *Trends Genet.* **19**, 321 (2003).
6. H. Masumoto, D. Hawke, R. Kobayashi, A. Verreault, *Nature* **436**, 294 (2005).
7. E. M. Hyland *et al.*, *Mol. Cell. Biol.* **25**, 10060 (2005).
8. A. Ozdemir *et al.*, *J. Biol. Chem.* **280**, 25949 (2005).
9. F. Xu, K. Zhang, M. Grunstein, *Cell* **121**, 375 (2005).
10. H. Zhou, B. J. Madden, D. C. Muddiman, Z. Zhang, *Biochemistry* **45**, 2852 (2006).
11. I. Celic *et al.*, *Curr. Biol.* **16**, 1280 (2006).
12. N. L. Maas, K. M. Miller, L. G. Defazio, D. P. Toczyski, *Mol. Cell* **23**, 109 (2006).
13. J. Recht *et al.*, *Proc. Natl. Acad. Sci. U.S.A.* **103**, 6988 (2006).
14. A. Sutton *et al.*, *J. Biol. Chem.* **278**, 16887 (2003).
15. D. T. Scholes, M. Banerjee, B. Bowen, M. J. Curcio, *Genetics* **159**, 1449 (2001).
16. R. Marmorstein, *Novartis Found. Symp.* **259**, 78 (2004).
17. N. J. Krogan *et al.*, *Nature* **440**, 637 (2006).
18. M. Lisby, U. H. Mortensen, R. Rothstein, *Nat. Cell Biol.* **5**, 572 (2003).
19. M. Lisby, R. Rothstein, U. H. Mortensen, *Proc. Natl. Acad. Sci. U.S.A.* **98**, 8276 (2001).
20. E. Shor, J. Weinstein, R. Rothstein, *Genetics* **169**, 1275 (2005).
21. J. C. Eissenberg, R. Ayyagari, X. V. Gomes, P. M. Burgers, *Mol. Cell. Biol.* **17**, 6367 (1997).
22. Z. Zhang, K. Shibahara, B. Stillman, *Nature* **408**, 221 (2000).
23. B. Suter *et al.*, *Genetics* **167**, 579 (2004).
24. A. H. Tong *et al.*, *Science* **303**, 808 (2004).
25. X. Pan *et al.*, *Cell* **124**, 1069 (2006).
26. R. D. Kolodner, C. D. Putnam, K. Myung, *Science* **297**, 552 (2002).
27. We thank H. M. Thompson, S. Kaufmann, J. Chen, C. McMurray, G. Isaya, and M. McNiven for editing and reading the manuscript and P. Burgers, R. Sternglanz, C. Wu, R. Rothstein, A. Bielinsky, and B. Stillman for reagents. Z.Z. expresses gratitude to B. Stillman for advice and support. This work was partly supported by grants from the NIH (Z.Z. and R.M.K.).

Supporting Online Material

www.sciencemag.org/cgi/content/full/315/5812/653/DC1
Materials and Methods
Figs. S1 to S8
Tables S1 and S2
References

31 July 2006; accepted 20 December 2006
10.1126/science.1133234

A Two–Amino Acid Change in the Hemagglutinin of the 1918 Influenza Virus Abolishes Transmission

Terrence M. Tumpey,[1]* Taronna R. Maines,[1] Neal Van Hoeven,[1] Laurel Glaser,[2] Alicia Solórzano,[2] Claudia Pappas,[1,2] Nancy J. Cox,[1] David E. Swayne,[3] Peter Palese,[2] Jacqueline M. Katz,[1] Adolfo García-Sastre[2]

The 1918 influenza pandemic was a catastrophic series of virus outbreaks that spread across the globe. Here, we show that only a modest change in the 1918 influenza hemagglutinin receptor binding site alters the transmissibility of this pandemic virus. Two amino acid mutations that cause a switch in receptor binding preference from the human α-2,6 to the avian α-2,3 sialic acid resulted in a virus incapable of respiratory droplet transmission between ferrets but that maintained its lethality and replication efficiency in the upper respiratory tract. Furthermore, poor transmission of a 1918 virus with dual α-2,6 and α-2,3 specificity suggests that a predominant human α-2,6 sialic acid binding preference is essential for optimal transmission of this pandemic virus. These findings confirm an essential role of hemagglutinin receptor specificity for the transmission of influenza viruses among mammals.

The "Spanish" influenza pandemic virus spread globally and resulted in the deaths of up to 50 million people worldwide (*1*, *2*). The ability of this H1N1 pandemic strain to spread rapidly and cause high rates of illness among humans makes it valuable for studying the molecular properties that confer efficient transmissibility of influenza viruses. An influenza virus bearing all eight gene segments of the 1918 pandemic virus was recently generated in cultured cells, was found to be lethal for chicken embryos and mice, and displayed a high-growth phenotype in human lung cells. Furthermore, the 1918 hemagglutinin (HA) and polymerase genes were shown to be essential for maximal virus replication and optimal virulence (*3*–*5*).

Influenza pandemics seem to occur every 10 to 40 years, but the factors that lead to the emergence of pandemic viruses are complex and poorly understood. However, the establishment of efficient and sustained human-to-human transmission of a virus to which humans have

[1]Influenza Branch, Mailstop G-16, Division of Viral and Rickettial Diseases, National Center for Infectious Diseases, Centers for Disease Control and Prevention, 1600 Clifton Road NE, Atlanta, GA 30333, USA. [2]Department of Microbiology, Mount Sinai School of Medicine, New York, NY 10029, USA. [3]Southeast Poultry Research Laboratory, Agricultural Research Laboratory, U.S. Department of Agriculture, 934 College Station Road, Athens, GA 30606, USA.

*To whom correspondence should be addressed. E-mail: tft9@cdc.gov